materials proceedings

MDPI

Proceeding Paper

The Influence of Adding a Functionalized Fluoroalkyl Silanes (PFDTES) into a Novel Silica-Based Hybrid Coating on Corrosion Protection Performance on an Aluminium 2024-t3 Alloy †

Magdi H. Mussa [1,2,3,*], Yaqub Rahaq [3], Sarra Takita [3], Farah D. Zahoor [3,4], Nicholas Farmilo [3,5] and Oliver Lewis [3]

1 Mechanical and Energy Department, The Libyan Academy of Graduate Study, Tripoli P.O. Box 79031, Libya
2 Mechanical Engineering Department, Sok Alkhamis Imsehel High Technical Institute, Sok Alkhamis, Tripoli P.O. Box 79033, Libya
3 Material and Engineering Research Institute (MERI), Sheffield Hallam University, Sheffield S1 1WB, UK; yakoobsameer111@gmail.com (Y.R.); sarah.a.takita@gmail.com (S.T.); F.Zahoor@sheffield.ac.uk (F.D.Z.); nfarmilo@gmail.com (N.F.); O.Lewis@shu.ac.uk (O.L.)
4 Department of Chemistry, University of Sheffield, Brook Hill, Sheffield S3 7HF, UK
5 Tideswell Business Development Ltd., Ravensfield Sherwood Rd., Buxton SK17 8HH, UK
* Correspondence: magdimosa1976@gmail.com; Tel.: +44-7404496955
† Presented at the 2nd International Online Conference on Polymer Science—Polymers and Nanotechnology for Industry 4.0, 1–15 November 2021; Available online: https://iocps2021.sciforum.net/.

Abstract: Silica-based coatings prepared using sol-gel polymerizing technology have been shown to exhibit excellent chemical stability combined with reducing the corrosion of metal substrates, showing promising use in aerospace and marine applications to protect light alloys. Moreover, this technology is an eco-friendly technique route for producing surface coatings, showing high potential for replacing toxic pre-treatment coatings of traditional conversation chromate coatings. This study aims to investigate the enhancement in corrosion protection of a hybrid-organic-inorganic silica-based coating cured at 80 °C by increasing the hydrophobicity to work on the aluminium 2024-T3 alloy. This approach involving a novel silica-based hybrid coating was prepared by introducing 1H,1H,2H,2H-perfluorodecyltriethoxysilane (PFDTES) into the base hybrid formula created from tetraethylorthosilicatesilane (TEOS) and triethoxymethylsilane (MTMS) precursors; this formula was enhanced by introducing a Polydimethylsiloxane polymer (PDMS). The corrosion protection properties of these coatings were examined by being immersed in 3.5% NaCl with electrochemical impedance testing (EIS) and Potentiodynamic polarization scanning (PDPS). The chemical elements confirmation was performed using infrared spectroscopy (ATR-FTIR); all this was supported by analysing the surface morphology before and after the immersion by using scanning electron microscopy (SEM). The results of the electrochemical impedance testing analyses reveal the new open finite-length diffusion circuit element due to electrolyte media diffusion prevented by fluorinated groups. Additionally, it shows increases in corrosion protection arising from the increasing hydrophobicity of the fluorinated coating compared to other formulas cured under similar conditions and bare substrate. Additionally, the modified sol-gel exhibited improved resistance to cracking, while the increased hydrophobicity may also promote self-cleaning.

Keywords: silica-based hybrid sol-gel coating; electrochemical testing; corrosion protection; aluminium alloys

Citation: Mussa, M.H.; Rahaq, Y.; Takita, S.; Zahoor, F.D.; Farmilo, N.; Lewis, O. The Influence of Adding a Functionalized Fluoroalkyl Silanes (PFDTES) into a Novel Silica-Based Hybrid Coating on Corrosion Protection Performance on an Aluminium 2024-t3 Alloy. *Mater. Proc.* **2021**, *7*, 6. https://doi.org/10.3390/IOCPS2021-11240

Academic Editor: Shin-ichi Yusa

Published: 30 October 2021

1. Introduction

The hybrid silica-based derived coatings have already been identified as a potential solution for the aerospace and marine industry in terms of corrosion protection [1–3]. The

sol-gel process is an eco-friendly method of surface protection, which offers many options, including using single- or multi-layer coating systems with anti-corrosion and antifouling systems [2,4–6]. Additionally, sol-gel coatings can present other desirable properties, such as preventing ice accumulation, oxidation resistance and abrasion resistance [7–9]. Nevertheless, long-term exposure to moisture can negatively influence many coatings systems' adhesion and cohesion properties [4,10]. Hydrophobicity has a pivotal role in reducing the adhesion between the surfaces and direct electrolyte exposure, reducing the diffusion in coatings' pores. The precursor 1H,1H,2H,2H-Perfluorodecyltriethoxysilane (PFDTES), as shown in Figure 1, is used for hydrophobicity polyvinylidene fluoride (PVDF) to protect the metal surfaces from fouling and biocorrosion, while being reasonably cost-effective, which potentially can be used to create anti-icing and anti-corrosion surfaces [11,12].

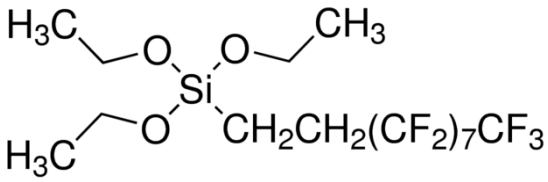

Figure 1. Chemical structure of 1H,1H,2H,2H-Perfluorodecyltriethoxysilane (PFDTES) precursor.

In this study, the performance of a functionalized silica-based sol-gel coating by introducing a 1H,1H,2H,2H-Perfluorodecyltriethoxysilane (PFDTES) precursor was investigated against corrosion by utilizing 3.5% NaCl to simulate the extended exposure similar to applications.

2. Experimental Work

2.1. Substrate Preparation

Q-panels were supplied by Q-Lab made of aluminium alloy AA2024 T3 with dimensions 102 mm × 25 mm × 1.6 mm for use as test substrates [13]. The acetone was used to remove organic residues such as grease oils or fats present on the substrate and then placed in an ultrasonic water bath for 5 min for additional cleaning with a standard alkaline solution cleaner, followed by rinsing deionized water (DI) and nitrogen drying.

2.2. Sol-Gel Preparation

The hybrid silica-based sol-gel was prepared by mixing tetraethylorthosilicate silane (TEOS), trimethoxymethyl silane (MTMS) and isopropanol (all purchased from Sigma-Aldrich (St. Louis, MO, USA)) and with dropwise additions of DI water at the molar ratio of 18:14:17:220, respectively. Then, it was enhanced by adding 12 mol% of Polydimethylsiloxane polymer (PDMS) solution. To complete the hydrolysing and the condensation polymerization reaction, the mixture was stirred with dropwise additions of nitric acid as a catalyst; the formulation was then stirred for 24 h [13]. This formula was used as the unmodified base coating and labelled as SHX. Next, the modified, fluorinated hybrid sol-gel, labelled as PF-SHX, was prepared by adding 1.5 vol.% of PFDTES from Sigma-Aldrich into the original SHX sol-gel formulation.

The formula was applied by spray coating the clean substrate and building it up over three passes. After that, the coated samples were left in the atmosphere for 10 min before being thermally annealed at 80 °C for 4 h—the chosen samples with a thickness of 16 ± 2 micrometre were chosen. Table 1 shows simple codes used to identify samples.

Table 1. Sample identification table.

No.	Identifier	Base Composite Sol-Gel	(PFDTES) *v*/*v*%	Curing Temperature
1.	SHX-80	TEOS + MTMS + PDMS	-	80 °C
2.	PF-SHX-80	TOES + MTMS + PDMS	1.5%	80 °C
3.	Bare AA2024 T3	-	-	-

3. Results and Discussion

3.1. Electrochemical Corrosion Testing

3.1.1. Potentiodynamic Polarization (PDPS)

Potentiodynamic polarization scans were performed on all the samples with hybrid sol-gel coatings. The results for SHX-80 and PF-SHX-80 are presented in Figure 2, along with the result of a test conducted on a bare 2024-T3 aluminium alloy for comparison. The values of corrosion potential (E_{corr}) and measured current density (I_{corr}) were obtained by extrapolating the cathodic and anodic curves using the Tafel extrapolation method. The results are shown in Table 2. The results show that the coatings reduced the measured current when compared to the uncoated aluminium alloy and shifted the corrosion potential to more noble values. This phenomenon was more apparent in the PF-SHX-80 coating, which showed a shift of 199 mV compared to the uncoated 2024-T3. The initial observation indicated that the corrosion protection offered by both sol-gel coatings is due to excellent barrier properties. Nevertheless, the shift in E_{corr} indicates that the anode is inhibited to a greater degree than the cathode; this is attributed to the fluorine-carbon atoms bridging to the substrate [14,15].

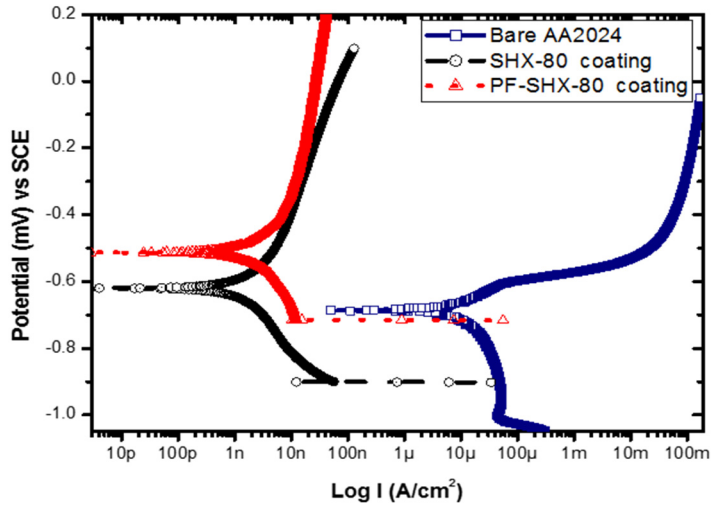

Figure 2. PDPS Polarization curves for the bare AA 2024-T3 alloy and sol-gel coated samples.

Table 2. Parameters obtained from Tafel extrapolation for bare AA 2024-T3, sol-gel coated samples.

Sample	E_{corr} [mV vs. SCE]	I_{corr} [A/cm^2]	OCP [mV vs. SCE]
Bare-AA 2024	-662 ± 2	7.10×10^{-6}	−640
SHX-80 coating	-608 ± 2	1.02×10^{-9}	−708
PF-SHX-80 coating	-521 ± 2	1.22×10^{-9}	−658

3.1.2. Electrochemical Impedance Spectroscopy (EIS) Analysis

Tests were performed over a period of 14 days. Figure 3a,b show Bode impedance magnitude plots for PF-SHX-80 and the SHX-80 coated samples and bare AA2024-t3 sample in the first hour and after 336 h.

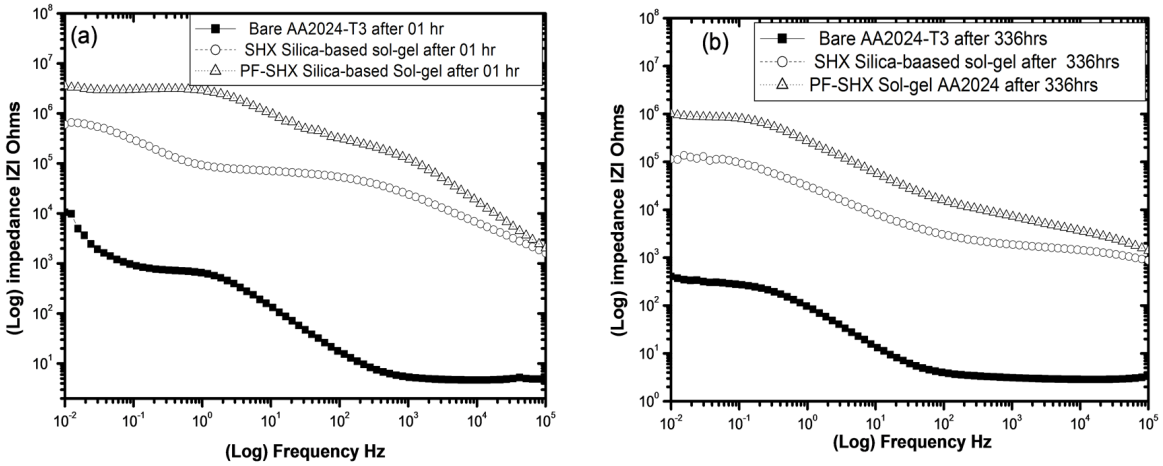

Figure 3. Bode Impedance magnitude plots for PF-SHX-80 and SHX-80 and bare samples (**a**) from 01 h and (**b**) after 336 h.

The overall impedance was increased by approximately one order of magnitude for the PF-SHX-80-coated samples compared to the SHX-80 samples, with impedance values of 6.8×10^6 and 6.8×10^5 Ω/cm^2, respectively, after one hour. At frequencies between 100 and 105 Hz, the impedance curve for the PF-SHX-80 sample reveals pure capacitive behaviour (C). Then, the impedance slowly increased from about 6.6×10^5 Ω/cm^2 in the middle range of the frequencies and finally reached a point where the rate of increase impedance is small at the low frequencies. Similarly, in the EIS measurements of the SHX-80-coated sample, a noticeable drop in impedance was observed at about 1.0×10^5 Ω/cm^2 after 14 days. On the other hand, this SHX coating still revealed higher impedance compared to the bare substrate. The increased R_{ct} values obtained from PF-SHX are consistent with the anodic inhibition obtained through a fluorine-influenced interface [15].

3.1.3. Electrochemical Equivalent Circuits Fitting for Both Sol-Gel Coatings

Tables 3 and 4 below demonstrate the fitted data obtained from the EIS spectra for the SHX-80 and the PF-SHX-80 sol-gel coatings. The equivalent circuits were used to simulate the corrosion mechanism on the coated sample in 01, 48 and 144 h. A time-constant element (Q) was used in these circuits instead of an ideal capacitor C to account for current leakage in the alternating current signals' capacitor and/or the frequency dispersion effect [14,16].

Table 3. The fitted data obtained from EIS spectra for the PF-SHX-80 sol-gel coating after various immersion times.

Sample	Element	Immersion Time (h)		
		01	**48**	**144**
	Circuit	R(Q(R(QR)))	R(Q(RO)(QR))	R(Q(RO)(RQ))
	R_s	10	18	45
	Q_{ct}	8.913×10^{-10}	9.326×10^{-10}	1.915×10^{-9}
	n	1	1	0.900
	R_{ct}	2.220×10^6	6.522×10^4	3.776×10^4
	O_{ct}	-	2.823×10^{-7}	4.866×10^{-7}
	B	-	0.469	0.618
	Q_{iL}	3.800×10^{-8}	1.103×10^{-7}	3.592×10^{-7}
	n	0.772	0.803	0.800
	R_{iL}	3.319×10^6	9.675×10^5	2.136×10^4

Table 4. The fitted data obtained from EIS spectra for the SHX-80 sol-gel coating after various immersion times.

Sample	Element	Immersion Time (h)		
		01	**48**	**144**
	Circuit	R(Q(R(QR)))	R(Q(R(Q(RW))))	R(Q(R(Q(RW))))
	R_s	100	205	195
	Q_{ct}	1.085×10^{-7}	2.059×10^{-7}	6.118×10^{-6}
	n	0.649	0.800	0.752
	R_{ct}	7.294×10^{4}	817	110
	Q_{iL}	4.934×10^{-6}	1.236×10^{-6}	9.815×10^{-6}
	n	0.827	0.800	0.818
	R_{iL}	7.790×10^{5}	3.504×10^{6}	1.475×10^{5}
	W	-	2.317×10^{-5}	8.084×10^{-5}

The elements used for the equivalent circuits were solution resistance (R_s), coating resistance (R_{ct}), coating constant phase elements (Q_{ct}), intermediate oxide layer resistance (R_{iL}), intermediate oxide layer capacitance (Q_{iL}), finite Warburg-circuit element (O) and Warburg-circuit element (W) [16].

At the first hour of immersion, both samples illustrate the same behaviour with three resistance and two time constants, respectively, as shown in Figure 4a,c. However, after 48 h of immersion of both coated samples, they started behaving individually. The SHX-80 coating's results indicate that there are three time constants. The first one arises in the high-frequency range and may be attributed to capacitive effects at the coating/aluminium/aluminium oxide interfacial layer in the coating, the second one is due to the diffusion properties of the coating, and the third one may be attributed to the Warburg-circuit element (W) as a result of diffusion to the substrate surface, as shown in Figure 4d. On the other hand, the PF-SHX-80-coated sample kept two time constants with a finite Warburg-circuit element (O) in the coating zone, as shown in Figure 4b. This (O) element is thought to originate from the hydrophobic nature of the fluorinated group ($-CH_2CH_2(CF2)_7CF_3$) from the PFDTES additive, which may prevent the diffusion of electrolyte into the fluorinated coating.

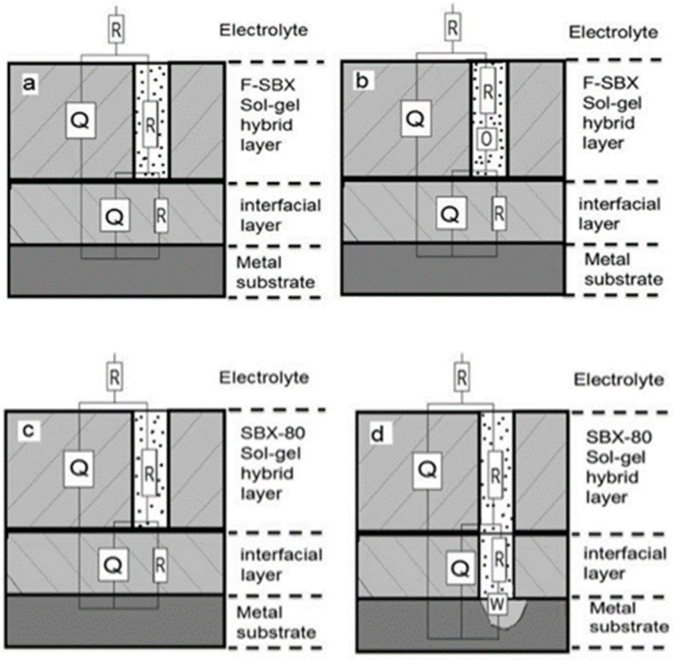

Figure 4. The modelling of (**a**,**b**) PF-SHX-80 and (**c**,**d**) SHX-80 coating systems.

3.2. Confirmation of PFDTES Addition in Sol-Gel Formula

The successful integration of the fluorinated functional groups from the (PFDTES) precursor into the sol-gel was confirmed by comparing the infrared spectrum obtained from the PF-SHX-80 coating to the unmodified SHX-80, as shown in Figure 5. The presence of C-F bonds can be confirmed in the spectral range between 1400 and 900 cm^{-1}; also, C-F_2 with C-F_3 bonds can be observed in the spectrum by the presence of bands at 1140 and 1250 cm^{-1}. The presence of the bands was highlighted with perpendicular lines on the spectrum of the based and modified sol-gels [17].

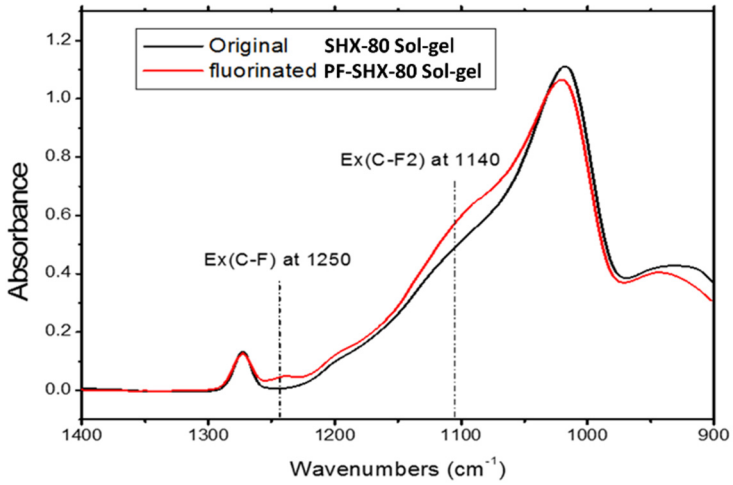

Figure 5. ATR-FTIR spectra showing the effect of PFDTES addition to the unmodified SBX-80 sol-gel.

3.3. Water Contact Angle Measurements of SHX-80- and PF-SHX-80-Coated Samples

Figure 6 shows a typical bar chart of the mean values of the water contact angle measurement droplets on both coating systems. The result of the measured average water contact angle (WCA) of the original SHX-80 coating was 67° ± 2°. The result of WCA on the modified PF-SHX-80 sol-gel coating was 118° ± 3°. The higher water contact angle recorded for the PF-SHX-80 shows that its wettability is lower than that of the SHX-80 as a result of the increased hydrophobicity of the fluorinated F-SBX-80 coating [18].

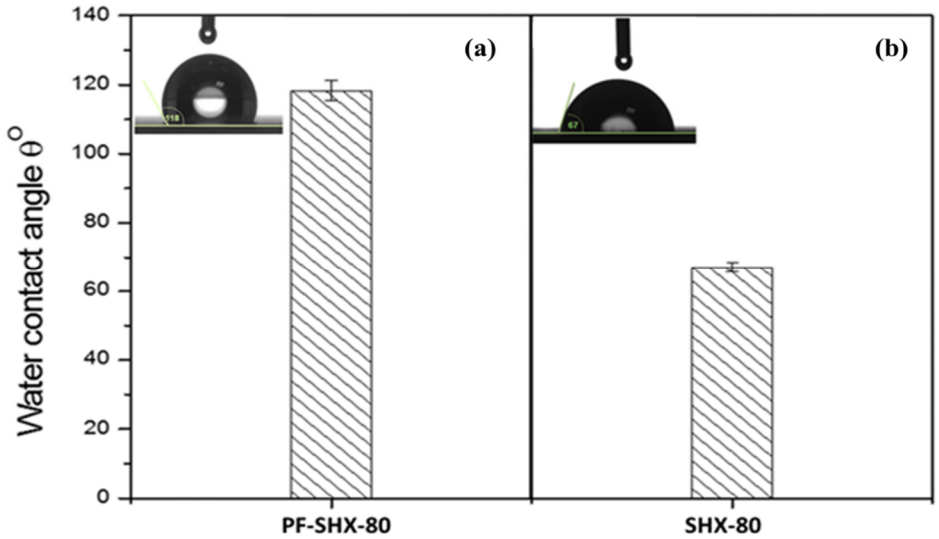

Figure 6. Bar chart showing the droplets and the mean values of WCA of (**a**) PF-SBX-80 and (**b**) SBX-80 coatings.

3.4. Scanning Electron Microscopy Imaging

Both coated samples SHX-80 and PF-SHX-80 demonstrated an ability to provide good barrier corrosion protection to the aluminium alloy substrate during long immersion. The visual examination of samples immediately after immersion showed no apparent degradation or damage to both coatings. Nevertheless, after longer immersion times (greater than ten days), the SHX-80 coating was susceptible to the formation of microcracks and pitting under the coating. The cracks were observed to be around 1–3 µm wide on the surface, as shown in the SEM images in Figure 7a. Since the presence of water under the film could lead to swelling and the loss of coating–substrate adhesion, leading to the cracking observed in the case of SHX-80. However, the PF-SHX-80 coating showed excellent resistance to cracking under similar circumstances, and this is attributable to the flexibility properties new coating, as shown in Figure 7b.

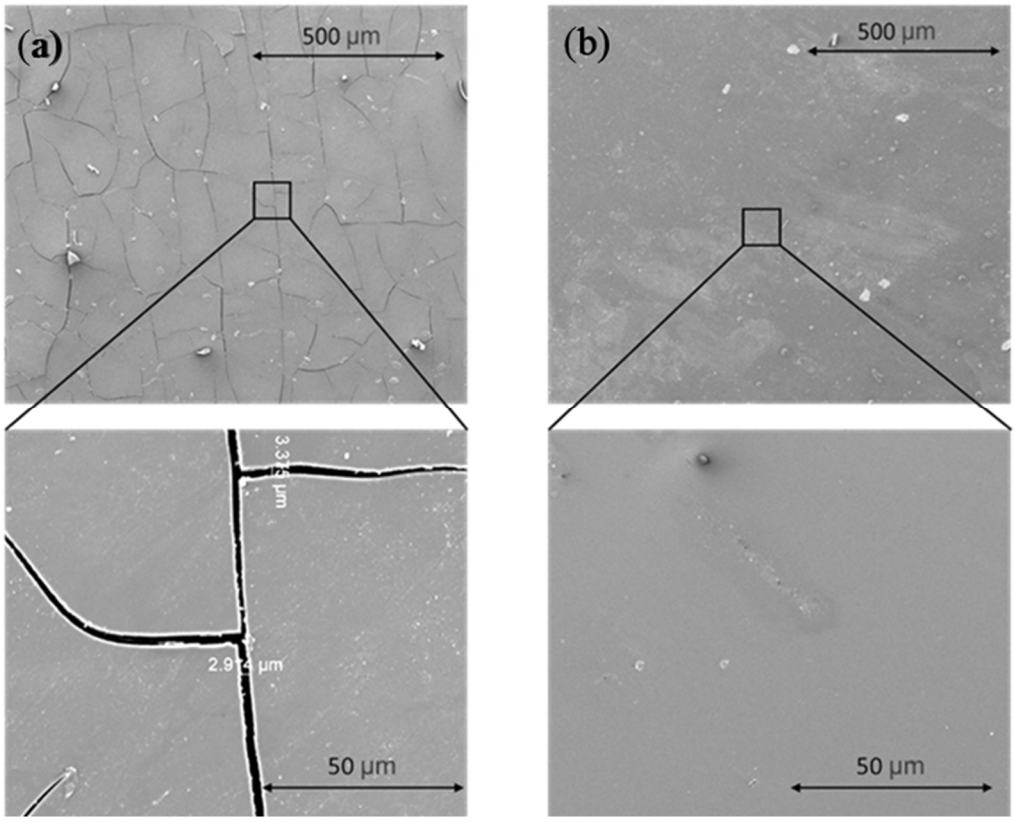

Figure 7. Secondary electron SEM micrographs of the long immersion effect on both coatings (**a**) SHX-80 and (**b**) PF-SHX-80.

4. Conclusions

The addition of the PFDTES precursor has the potential to enhance the corrosion performance of the basic TEOS and MTMS silica-based hybrid sol-gel coating on AA2024-T3 substrates. The electrochemical corrosion testing techniques confirm this by enhancing the hydrophobicity of the coating compared to other coatings with the same curing temperature of 80 °C. Furthermore, the fluorinated group from PFDTES in the hybrid organic-inorganic sol-gel coating exhibits improved post-exposure cracking resistance after prolonged immersion than the unmodified sol-gel coating. Moreover, exploiting the hydrophobic nature of the PFDTES precursor in low concentrations is potentially beneficial for applications that require self-cleaning, anti-icing or antifouling properties.

Author Contributions: Conceptualization, M.H.M.; methodology, M.H.M.; validation, M.H.M. and Y.R.; data analysis, M.H.M., S.T. and Y.R.; FTIR support, S.T. and F.D.Z.; investigation, M.H.M.; resources, M.H.M., O.L. and N.F.; writing—original draft preparation, M.H.M.; writing—review and editing, M.H.M., O.L. and N.F.; project supervision O.L. and N.F. All authors have read and agreed to the published version of the manuscript.

Funding: This research was funded by the Libyan scholarship program.

Institutional Review Board Statement: Not applicable.

Informed Consent Statement: Not applicable.

Data Availability Statement: The data are not publicly available; The data files are stored on corresponding instruments and on personal computers.

Acknowledgments: The authors would like to acknowledge the facilitating support by Sheffield Hallam University at Material and Engineering research institute MERI and also the Libyan Scholarship Program for the financial support.

Conflicts of Interest: The authors declare no conflict of interest.

References

1. Marks, D.L.; Vinegoni, C.; Bredfeldt, J.S.; Boppart, S.A. Interferometric differentiation between resonant coherent anti-Stokes Raman scattering and nonresonant four-wave-mixing processes. *Appl. Phys. Lett.* **2004**, *85*, 5787–5789. [CrossRef]
2. Detty, M.R.; Ciriminna, R.; Bright, F.V.; Pagliaro, M. Environmentally benign sol-gel antifouling and foul-releasing coatings. *Acc. Chem. Res.* **2014**, *47*, 678–687. [CrossRef] [PubMed]
3. Mussa, M.H.; Zahoor, F.D.; Lewis, O.; Farmilo, N. Developing a Benzimidazole-Silica-Based Hybrid Sol–Gel Coating with Significant Corrosion Protection on Aluminum Alloys 2024-T3. *Eng. Proc.* **2021**, *11*, 3. [CrossRef]
4. Wang, H.; Akid, R.; Gobara, M. Scratch-resistant anticorrosion sol–gel coating for the protection of AZ31 magnesium alloy via a low temperature sol-gel route. *Corros. Sci.* **2010**, *52*, 2565–2570. [CrossRef]
5. Chen, S.; Li, L.; Zhao, C.; Zheng, J. Surface hydration: Principles and applications toward low-fouling/nonfouling biomaterials. *Polymer* **2010**, *51*, 5283–5293. [CrossRef]
6. Eduok, U.; Suleiman, R.; Gittens, J.; Khaled, M.; Smith, T.J.; Akid, R.; Alia, B.; Khalile, A.; El Ali, B.; Khalil, A. Anticorrosion/antifouling properties of bacterial spore-loaded sol-gel type coating for mild steel in saline marine condition: A case of thermophilic strain of Bacillus licheniformis. *RSC Adv.* **2015**, *5*, 93818–93830. [CrossRef]
7. Lev, O.; Wu, Z.; Bharathi, S.; Glezer, V.; Modestov, A.; Gun, J.; Rabinovich, L.; Sampath, S. Sol-Gel Materials in Electrochemistry. *Chem. Mater.* **1997**, *9*, 2354–2375. [CrossRef]
8. Wang, D.; Bierwagen, G.P. Sol-gel coatings on metals for corrosion protection. *Prog. Org. Coat.* **2009**, *64*, 327–338. [CrossRef]
9. Pathak, S.S.; Khanna, S. Sol-gel nano coatings for corrosion protection. *Met. Surf. Eng.* **2012**, *12*, 304–329.
10. Zhang, S.; Xianting, Z.; Yongsheng, W.; Kui, C.; Wenjian, W. Adhesion strength of sol-gel derived fluoridated hydroxyapatite coatings. *Surf. Coat. Technol.* **2006**, *200*, 6350–6354. [CrossRef]
11. Merck 1H,1H,2H,2H-Perfluorodecyltriethoxysilane 97%. Available online: https://www.sigmaaldrich.com/GB/en/product/aldrich/658758 (accessed on 22 June 2021).
12. Cui, X.-j.; Lin, X.-z.; Liu, C.-h.; Yang, R.-s.; Zheng, X.-w.; Gong, M. Fabrication and corrosion resistance of a hydrophobic micro-arc oxidation coating on AZ31 Mg alloy. *Corros. Sci.* **2015**, *90*, 402–412. [CrossRef]
13. Mussa, M. Development of Hybrid Sol-Gel Coatings on AA2024-T3 with Environmentally Benign Corrosion Inhibitors. Ph.D. Thesis, Sheffield Hallam University, Sheffield, UK, 2020.
14. Tait, W.S. *Electrochemical Impedance Spectroscopy Fundamentals, an Introduction to Electrochemical Corrosion Testing for Practicing Engineers and Scientists*; Tait, W.S., Ed.; PairODocs Publications: Racine, WI, USA, 1994; ISBN 13-978-0966020700.
15. Kobayashi, T.; Hugel, H.M. Special issue, organo-fluorine chemical science-inventing the fluorine future. In *Applied Sciences*; Multidisciplinary Digital Publishing Institute (MDPI): Basel, Switzerland, 2012; pp. 1–283, ISBN 3906980332.
16. Yabuki, A.; Yamagami, H.; Noishiki, K. Barrier and self-healing abilities of corrosion protective polymer coatings and metal powders for aluminum alloys. *Mater. Corros.* **2007**, *58*, 497–501. [CrossRef]
17. Brassard, J.; Sarkar, D.K.; Perron, J. Fluorine Based Superhydrophobic Coatings. *Appl. Sci.* **2012**, *2*, 453–464. [CrossRef]
18. Kumar, D.; Wu, X.; Fu, Q.; Ho, J.W.C.; Kanhere, P.D.; Li, L.; Chen, Z. Development of durable self-cleaning coatings using organic-inorganic hybrid sol-gel method. *Appl. Surf. Sci.* **2015**, *344*, 205–212. [CrossRef]